

Figure S1. POS-1(80-180) binds the *glp-1* fragment with a similar affinity to that of POS-1 1-206. Top, gel shift image labeled with the POS-1 concentrations (top) in each lane, and the RNA sequence beneath. The reported $K_{d,app}$ is the average \pm the standard deviation of six separate replicates. Bottom, representative fit of gel shift data to the Hill Equation.

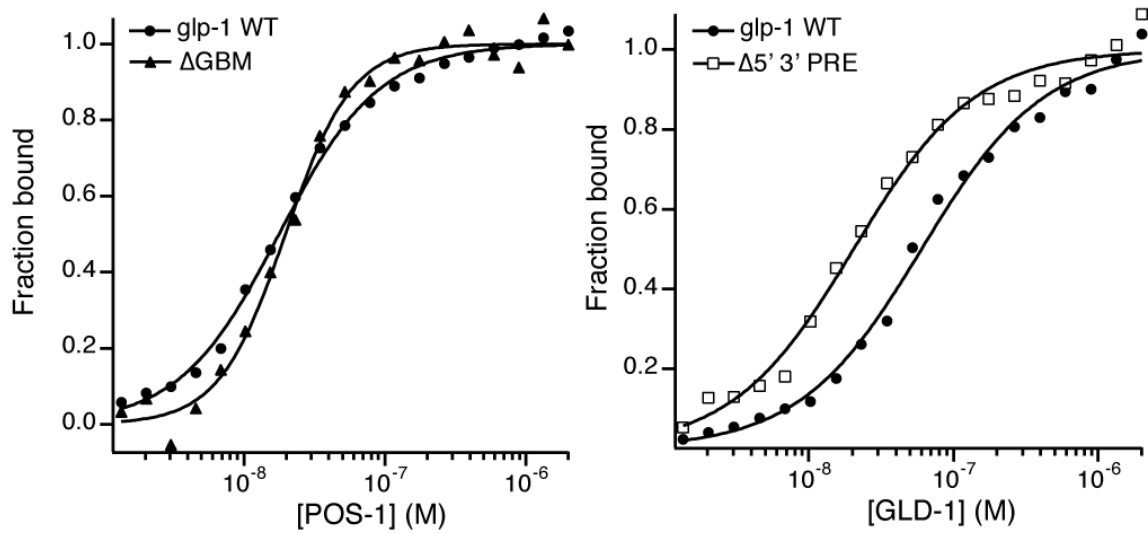


Figure S2. POS-1 or GLD-1 specific mutations in the *glp-1* 3' UTR. Left, representative EMSA fits for POS-1(1-206) binding to *glp-1* WT RNA (filled circles, $K_{d,app} = 19 \pm 2$ nM) and Δ GBM RNA (filled triangles, $K_{d,app} = 21 \pm 1$ nM). Right, representative EMSA fits for GLD-1(135-329) binding to *glp-1* WT RNA (filled circles, $K_{d,app} = 70 \pm 10$ nM) and Δ 5' 3' PRE RNA (open squares, $K_{d,app} = 20 \pm 4$ nM). Reported $K_{d,app}$ values are means \pm one standard deviation of three independent replicates.

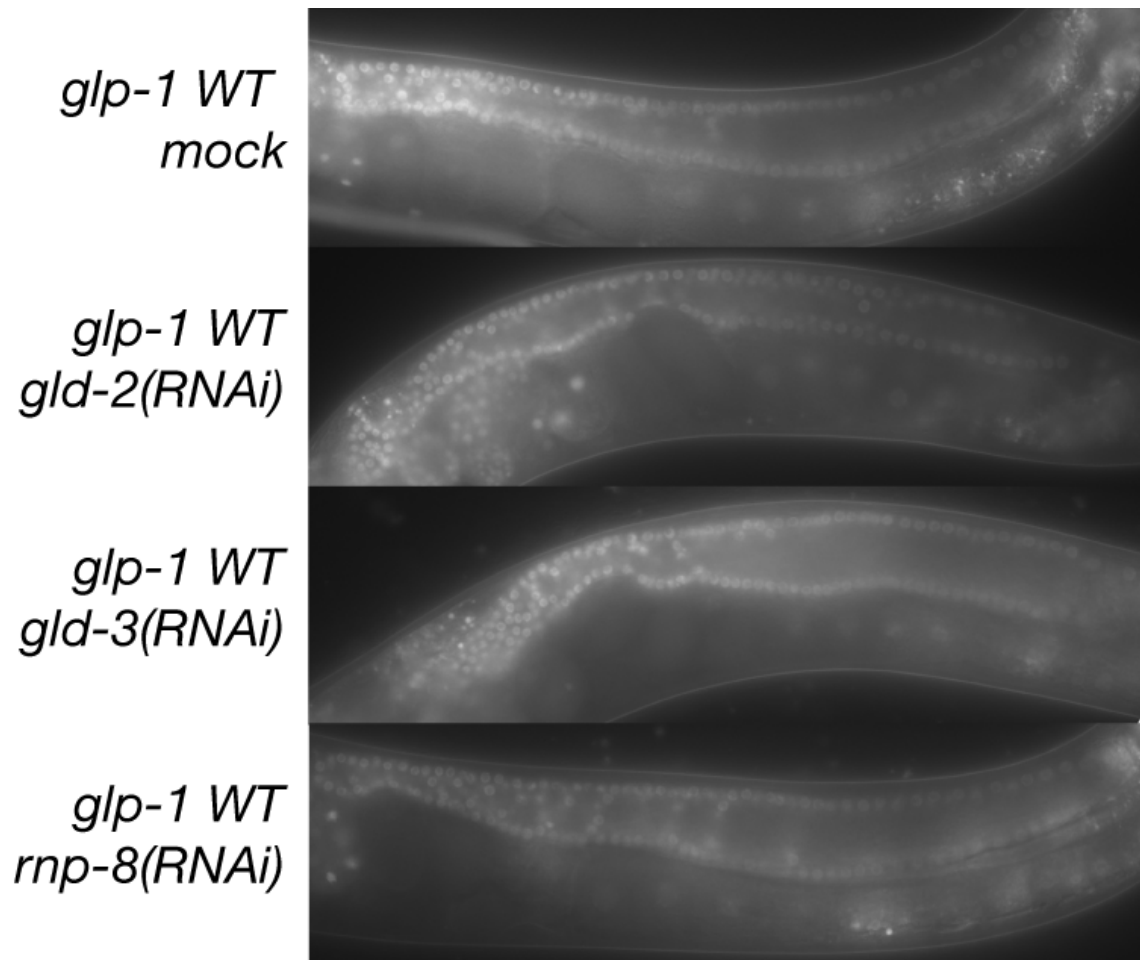


Figure S3. GLD-2 cytoplasmic poly(A) polymerase complexes are not required for translational activation of *glp-1* mRNA in the distal germline. Representative widefield fluorescence images for each of the listed experimental conditions. Each image is oriented with the distal most point of the germline at the upper left.